

상간리액터 없는 병렬연결 듀얼컨버터 시스템의 동작해석과 새로운 전류제어

論 文
49B-7-6

Operation Analysis and New Current Control of Parallel Connected Dual Converter System without Interphase Reactors

池 俊 根*
(Jun-Keun Ji)

Abstract - In this paper, a predictive current control of 12-pulse parallel connected dual converter system without interphase reactors(IPR) is presented. Firstly, the characteristics of system without IPR are analyzed and compared with that of system with IPR. And the predictive current control of this system is discussed. Finally the validity of the presented system and the excellence of the predictive current control response is proved through the simulation results and experimental results.

Key Words : Parallel connected dual converter, Predictive current control, Interphase reactors(IPR)

1. Introduction

The increasing size of electrochemical and electrometallurgical plant for manufacturing such products as chlorine, aluminum and copper, requires AC-DC power converters capable of delivering direct currents of up to 100kA, and sometimes higher. This necessitates multiple paralleling of semiconductor devices within the rectifier circuit and paralleling complete circuits. It is useful to use as high a pulse number as is economical to minimize both the ripple in the DC output voltage and the harmonic content in the AC supply current waveform to the rectifier installation. For example, 12-pulse operation is provided by supplying two parallel 6-pulse rectifiers with 30 degrees displaced AC voltages. A 24-pulse arrangement requires four 6-pulse rectifiers mutually phase displaced by 15 degrees. A disadvantage of high pulse number is the increased size and cost of the rectifier transformer arrangement to provide the necessary phase displacement. In standard practice, the transformer tank also encloses the center-tapped inductor, usually

known as an interphase reactor(IPR) or interphase transformer (IPT), connected between each pair of rectifier circuits, and circuit pairs if appropriate, on the DC side. This device prevents interaction between the rectifiers by sustaining the instantaneous voltage difference in their outputs caused by the phase displacement on the AC side. Nowadays, it is usually considered most economical to use a 12-pulse system. Therefore, the operation of 12-pulse parallel connected three-phase dual converter system with a 30 degrees phase displacement is considered. The size and cost of an IPR connected between converter circuits in electrochemical plant is such that, on economic grounds, it has occasionally been omitted.[1]

In this paper, it is proposed that 12-pulse parallel connected dual converter system without interphase reactors(IPR) to improve large size and cost problem. It is described that the operation analysis of 12-pulse parallel connected dual converter system without interphase reactors(IPR). And new high performance instantaneous current control method using predictive current control instead of PI average current control method is applied to this system. Using this proposed system using predictive current control method, it is possible to implement a high performance and large capacity DC motor drive system without IPR for industrial plant.

* 正 會 員 : 順天鄉大 工大 情報技術工學部 助教授 · 工博
接受日字 : 1999年 11月 29日
最終完了 : 2000年 6月 1日

2. 12-Pulse Parallel Connected Dual Converter System

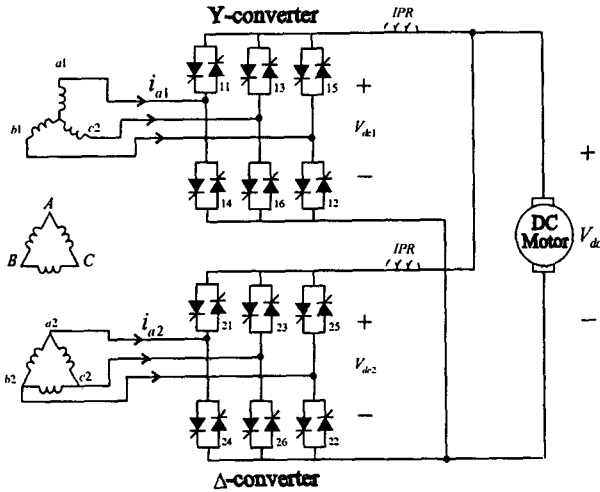


Fig. 1 12-pulse parallel connected dual converter system

Fig. 1 shows a schematic diagram of the 12-pulse parallel connected dual converter system supplied by two separate transformer output windings (the secondary and tertiary) with equal open-circuit voltages, and with the AC voltages in Δ -converter lagging that of Y-converter by 30 degrees. The number of turns per phase on the star-connected secondary windings is $1/\sqrt{3}$ times that on delta-connected tertiary windings. The primary windings has a delta connection. This provides higher output ripple frequency and minor improvement in input power factor. The position of a conventional IPR is shown in broken lines, although in this investigation it is omitted.[1]

The 12-pulse DC output is applied to the DC motor load. If the AC side inductances are assumed to be zero and without IPR, only the bridge converter which experiences the highest instantaneous voltage in any 12-pulse ripple period of 30 degrees will conduct. Thus the normal conduction interval of 120 degrees for a thyristors in one bridge converter is broken up by the conduction of thyristors in the other bridge converter. With the AC side inductances present, instantaneous transfer of load current between the bridge converters (and between phases within a bridge converter) is impossible, and commutation effects occur in various degrees of complexity.

3. Operation Analysis in case without IPR

To analyze operation in case without IPR, assuming that an inductance of loadside is extremely large, voltage and current waveforms are shown in Fig. 2. In this

figure, i_{a1} is an equivalent a-phase input current of Y-converter seen at the primary side of transformer and $i_{a1} = \frac{1}{\sqrt{3}} (i_{a1} - i_{c1})$. i_A is a A-phase input current at the primary side of transformer and $i_A = i_{a2} + i_{a1}$. A converter output voltage is given as equation (1).

$$V_{dc} = \max (V_{dc1}, V_{dc2}) \quad (1)$$

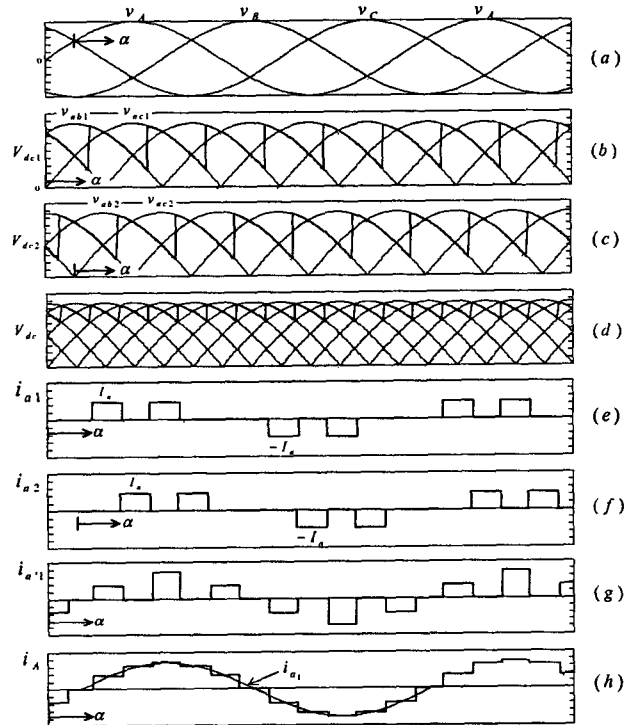


Fig. 2 Voltage and current waveforms of 12-pulse parallel connected converter system without IPR

Because the outputs of Y/ Δ -converter are directly connected to loadside, a load current flows through the converter in which an instantaneous output voltage is larger and the output current of Y/ Δ -converters is operated by 30 degrees discontinuously respectively. Assuming that the reference point of delay angle is same in cases with IPR and without IPR, The phase of input current in case without IPR is advanced 15 degrees compared with the case with IPR.[2][3]

3.1 Power factor

An important performance parameter of phase-controlled converter systems is the variation of supply power factor. The power factor is defined as[4]

$$PF = \frac{I_{A1}}{I_A} \cos \phi_1 = \mu \cos \phi_1 \quad (2)$$

To obtain the power factor, one must determine fundamental current and displacement angle. Primary input fundamental current is following:

$$I_{A_1} \angle \phi_1 = I_{a_2} \angle \phi_{a_2} + I_{a'1} \angle \phi_{1_1} \quad (3)$$

To calculate this in case with IPR, it is given as follows[3]:

$$I_{A_1} \angle \phi_1 = \frac{\sqrt{6}}{\pi} \angle -\alpha = 0.7797 \angle -\alpha \quad (4)$$

At the same manner, in case without IPR, it is given as follows:

$$\begin{aligned} I_{A_1} \angle \phi_1 &= \frac{4\sqrt{6}}{\pi} \sin \frac{\pi}{12} \angle \left(\frac{\pi}{12} - \alpha \right) \\ &= 0.8072 \angle \left(\frac{\pi}{12} - \alpha \right) \end{aligned} \quad (5)$$

And the rms input current can be determined from the resultant input current waveform as follows:

$$I_A = \left(\frac{2}{\pi} \int_a^{a+\pi} i_A d\theta \right)^{1/2} \quad (6)$$

To calculate this, it is 0.7885 in case with IPR and 0.8165 in case without IPR respectively. From this values the power factors in case with IPR and in case without IPR are given as equation (7) and (8) respectively.

$$PF_{IPR} = 0.9886 \cos \alpha \quad (7)$$

$$PF_{NO.IPR} = 0.9886 \cos \left(\alpha - \frac{\pi}{12} \right) \quad (8)$$

Therefore it is shown that the maximum value of power factor in two cases is same and the phase difference of 15 degrees only exists.

4. Predictive Current Control[5-7]

Firstly, we define input voltages for calculation needed to implement predictive current controller. If the rms value of primary line voltage in the transformer is assumed as E_{rms} , primary phase voltages and primary line voltages of transformer are defined as following.

$$\begin{aligned} V_A &= \frac{\sqrt{2}}{\sqrt{3}} E_{rms} \sin \omega t \\ V_B &= \frac{\sqrt{2}}{\sqrt{3}} E_{rms} \sin \left(\omega t - \frac{2}{3} \pi \right) \end{aligned} \quad (9)$$

$$\begin{aligned} V_C &= \frac{\sqrt{2}}{\sqrt{3}} E_{rms} \sin \left(\omega t + \frac{2}{3} \pi \right) \\ V_{AB} &= \sqrt{2} E_{rms} \sin \left(\omega t + \frac{\pi}{6} \right) \end{aligned}$$

$$V_{BC} = \sqrt{2} E_{rms} \sin \left(\omega t - \frac{2}{3} \pi + \frac{\pi}{6} \right) \quad (10)$$

$$V_{CA} = \sqrt{2} E_{rms} \sin \left(\omega t + \frac{2}{3} \pi + \frac{\pi}{6} \right)$$

Accordingly secondary line voltage of Y-transformer and tertiary line voltage of Δ -transformer are defined as following respectively.

$$\begin{aligned} V_{abl} &= \frac{1}{\sqrt{3}} (V_{AB} - V_{BC}) \\ V_{bcl} &= \frac{1}{\sqrt{3}} (V_{BC} - V_{CA}) \end{aligned} \quad (11)$$

$$\begin{aligned} V_{cal} &= \frac{1}{\sqrt{3}} (V_{CA} - V_{AB}) \\ V_{a2a2} &= V_{AB} \\ V_{b2b2} &= V_{BC} \\ V_{c2c2} &= V_{CA} \end{aligned} \quad (12)$$

The voltages applied to the loadside becomes the parts of these line voltages. The conducting thyristor of each bridge converter and loadside voltages are defined as Table 1 according to 12 conducting mode.(The number of each thyristor in the positive direction converters is designated in Fig. 1.)

Table 1 Loadside voltages and the number of conducting thyristor in each mode
(Y : Y-transformer, Δ : Δ -transformer)

Mode	1	2	3	4	5	6	7	8	9	10	11	12
U_d	$V_{abl} V_{ab2}$	$V_{ac1} V_{ac2}$	$V_{bc1} V_{bc2}$	$V_{ba1} V_{ba2}$	$V_{ca1} V_{ca2}$	$V_{cb1} V_{cb2}$						
Y	16	11	12	13	14	15						
	11	12	13	14	15	16						
Δ		26	21	22	23	24	25					
		21	22	23	24	25	26					

The equivalent circuit of converter system in steady state can be represented as Fig. 3. From this equivalent circuit, the voltage equation in each mode can be written as following.

$$R_a i_{dc} + \omega L_a \frac{di_{dc}}{d\omega t} + E_g = u_d \quad (13)$$

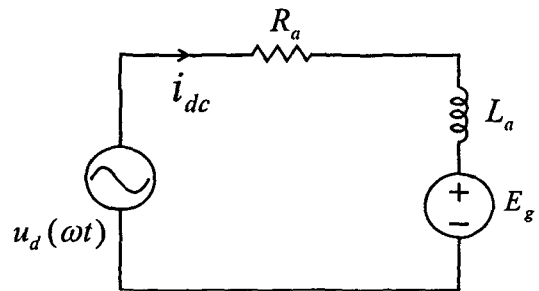


Fig. 3 Equivalent circuit in steady state

Where, u_d is an equivalent converter output voltage and becomes the part of sinusoidal line voltages as seen in Table 1. So the solution of this equation can be given as Eq. (14).

$$i_{dc} = I_1 \cos(\omega t - \phi) + I_2 e^{-\rho \omega t} + I_3 \quad (14)$$

Where, $\phi = \tan^{-1}\left(\frac{\omega L_a}{R}\right)$, $\rho = \frac{R_a}{\omega} L_a$,

$$Z = \sqrt{R_a^2 + (\omega L_a)^2}, \quad I_1 = \frac{u_{dmax}}{Z},$$

$$I_3 = -\frac{E_g}{R_a}, \quad u_{dmax} = \sqrt{2} E_{rms}$$

In Eq (14), I_2 can be solved differently as following according to continuous current or discontinuous current. For the sake of ease of calculation, we assume the case of mode 12. In mode 12, loadside voltage or motor input voltage can be represented as Eq. (15) by means of Table 1, Eq. (10) and (12).

$$u_d = u_{dmax} \cos \omega t \quad (15)$$

4.1 The Solution in Continuous Current Mode

From the condition which the average value of current for one period must be same as the reference current I^* ,

$$\begin{aligned} I^* &= \frac{6}{\pi} \int_a^{a+\frac{\pi}{6}} i_{dc} d\omega t \quad (16) \\ &= \frac{6}{\pi} \int_a^{a+\frac{\pi}{6}} [I_1 \cos(\omega t - \phi) + I_2 e^{-\omega \rho t} + I_3] d\omega t \end{aligned}$$

Arranging this equation to solve ,

$$I_2 = \frac{\pi}{6} [I^* - I_3 - \frac{12}{\pi} I_1 \sin \frac{\pi}{12} \cos(\alpha + \frac{\pi}{12} - \phi)] \frac{\rho e^{\rho \alpha}}{1 - e^{-\rho \frac{\pi}{6}}} \quad (17)$$

Where, α can be given from the condition which the average value of converter output voltage for one period must be satisfied.

$$\begin{aligned} V_{dc} &= \frac{6}{\pi} \int_a^{a+\frac{\pi}{6}} u_d d\omega t \\ &= \frac{6}{\pi} \int_a^{a+\frac{\pi}{6}} u_{dmax} \cos \omega t d\omega t \\ &= \frac{12}{\pi} u_{dmax} \sin \frac{\pi}{12} \cos(\alpha + \frac{\pi}{12}) \\ &= R_a I^* + E_g \quad (18) \end{aligned}$$

Therefore, α is represented as Eq. (19).

$$\alpha = -\frac{\pi}{12} + \cos^{-1}\left(\frac{R_a I^* + E_g}{V_{dcmax}}\right) \quad (19)$$

Where, $V_{dcmax} = \frac{12}{\pi} u_{dmax} \sin \frac{\pi}{12}$

4.2 The Solution in Discontinuous Current Mode

In discontinuous current mode, the integration interval for the average value of current becomes different according to extinction angle. If we assume the firing angle as α and the extinction angle as β , the initial condition is same as Eq. (20). And from this, Eq. (21a) and (21b) can be given.

$$i_{dc}(\alpha) = i_{dc}(\beta) = 0 \quad (20)$$

$$i_{dc}(\alpha) = I_1 \cos(\alpha - \phi) + I_2 e^{-\rho \alpha} + I_3 = 0 \quad (21a)$$

$$i_{dc}(\beta) = I_1 \cos(\beta - \phi) + I_2 e^{-\rho \beta} + I_3 = 0 \quad (21b)$$

Where, arranging Eq. (21b) to eliminate ,

$$I_2 = [-I_3 - I_1 \cos(\beta - \phi)] e^{\rho \beta} \quad (22)$$

Substituting this in Eq. (21a), Eq. (23) is given.

$$I_1 \cos(\alpha - \phi) - [I_3 + I_1 \cos(\beta - \phi)] e^{\rho(\beta - \alpha)} + I_3 = 0 \quad (23)$$

And we can get one more equation about α and β from the condition which the average value of converter output voltage for one period must be satisfied.

$$\begin{aligned} V_{dc} &= \frac{6}{\pi} [\int_a^\beta u_d d\omega t + \int_\beta^{a+\frac{\pi}{6}} E_g d\omega t] \\ &= \frac{6}{\pi} [\int_a^\beta u_{dmax} \cos \omega t + \int_\beta^{a+\frac{\pi}{6}} E_g d\omega t] \\ &= \frac{6}{\pi} [u_{dmax} (\sin \beta - \sin \alpha) + E_g (\alpha + \frac{\pi}{6} - \beta)] \\ &= R_a I^* + E_g \quad (24) \end{aligned}$$

Finally, we can get the solutions of α and β using Newton-Raphson numerical method from nonlinear equations of Eq. (23) and (24). And then we can get I_2 from Eq. (22) using the solutions.

5. Simulation Results

Motor parameters used in the simulation are same as Table 2 and the actual values of motor used in the experiments.

Table 2 Motor parameters

Rating Power	22[kW]
Rating Voltage	220[V]
Rating Current	90[A]
Amature Resistance R_a	0.35[Ω]
Amature Inductance L_a	6.5[mH]

Simulation Results are shown in Fig. 4. Fig. 4(a) shows the motor-side current waveforms (reference current : i^* , predictive current : $ipre$, motor current : idc) of continuous current mode in case of reference current reversal(50A and -50A). From this figure, it is

shown that motor current i_{dc} follows the reference current i^* very well with no overshoot.

The waveform of represented by dotted line is predictive current i_{pre} and gating signal is applied at the point that predictive current i_{pre} crosses motor current i_{dc} . It is also shown that the motor current follows desired current trajectory after gating signal applied. Fig. 4(b) also shows the motor-side current waveforms of discontinuous current mode in case of reference current reversal(1A and -1A) and it is shown that motor current i_{dc} follows the reference current i^* very well with no overshoot even discontinuous current mode.

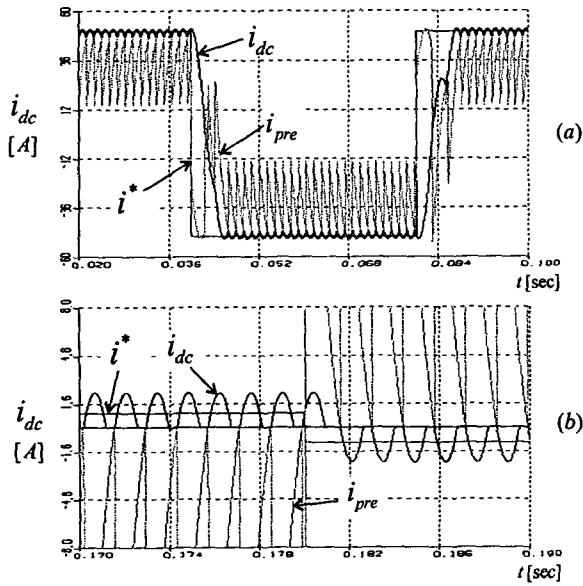


Fig. 4 Simulation current waveforms

6. Experimental Results

Experimental Results are shown in Fig. 5 and 6. Fig. 5 shows the current and voltage waveforms(reference current : i_{dc_ref} , motor current : i_{dc} , Y-converter current : i_{dc_1} , Δ -converter current : i_{dc_2} , motor voltage : V_{dc} , Y-converter predictive current : i_{pre1} , Δ -converter predictive current : i_{pre2}) of continuous current mode in case of reference current reversal(30A and -30A). From this figure, it is shown that motor current i_{dc} follows the reference current i_{dc_ref} very well with no overshoot and is same as the sum of i_{dc1} and i_{dc2} . Fig. 6 also shows the current and voltage waveforms of discontinuous current mode in case of reference current reversal(2A and -2A) and it is shown that motor current i_{dc} follows the reference current i_{dc_ref} very well with no overshoot even discontinuous current mode and is also same as the sum of i_{dc1} and i_{dc2} .

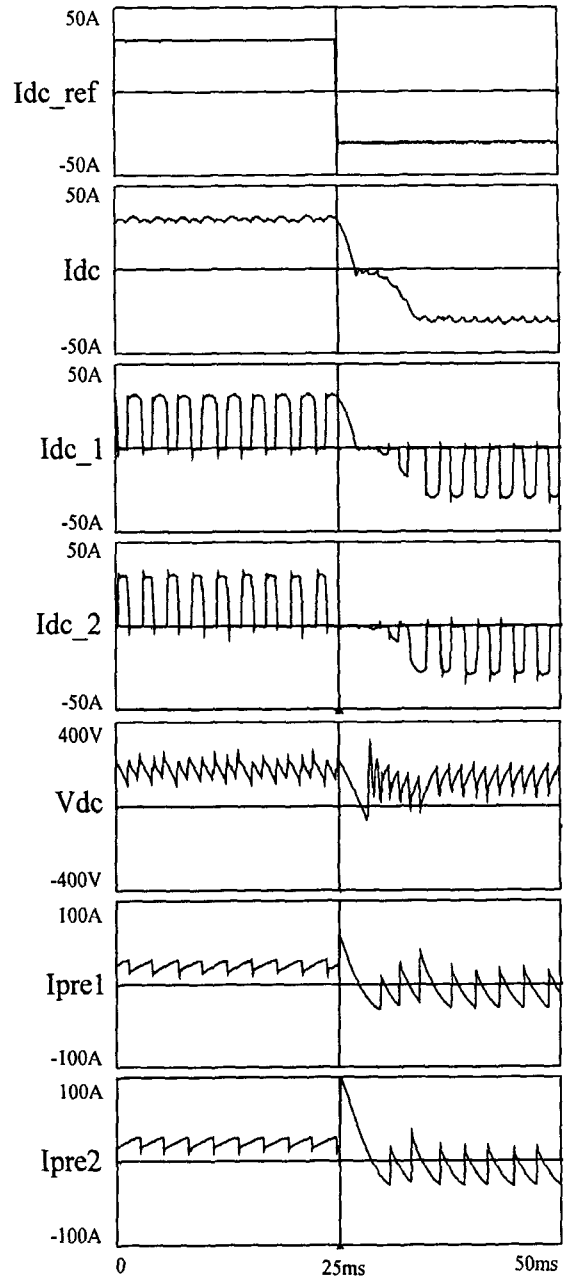


Fig. 5 Predictive current control response in continuous current mode (30A and -30A)

7. Conclusion

In this paper the characteristics of 12-pulse parallel connected dual converter system without interphase reactors(IPR) are analyzed and compared with that of system with IPR. And applying the predictive current control in this system, we can implement the high performance DC drive system having fast and accurate current control response besides getting economic advantage through removing IPR. Finally the validity of

References

- [1] Hall, J. K., Kettleborough, J. G., and Razak, A.B. M. J., "Parallel operation of bridge rectifiers without an interbridge reactor", Proc. IEE Pt. B, vol. 137, no. 2, pp. 125-140, 1990.
- [2] Ned Mohan, Tore M. Underland and William P. Robbins, Power Electronics, John Wiley & Sons, Inc., 2nd Edition, 1995.
- [3] Thomas H. Barton, Rectifiers, Cycloconverters, and AC Controllers, Oxford University Press, 1994.
- [4] Paresh C. Sen, Thyristor DC Drives, John Wiley & Sons, Inc., 1980.
- [5] 지준근, 설승기, 박민호, 김기택, 김경환, "예측 전류 제어를 사용하는 압연용 직류전동기 구동 시스템," 대한전기학회 논문지, 제 41권 12호, pp. 1387~1396, 1992.
- [6] Jun-Keun Ji, Seung-Ho Song, Seung-Ki Sul, Min-Ho Park, "DSP Based Self-Tuning IP Speed Controller and Predictive Current Controller for Rolling Mill DC Drive," in Proc. of IEEE PCC(Power Conversion Conferece), Yokohama, pp. 303~308, 1993.
- [7] 박기태, 지준근, 설승기, 최장호, 신현석, 이창원, 장계용, "상간 리액터를 제거한 12상 병렬연결 듀얼 컨버터 시스템의 예측 전류 제어", 대한 전기학회 하계학술대회, pp. 482-485, 1996.
- [8] Jun-Keun Ji, Seung-Ki Sul, "Predictive Current Control of 12-Pulse Parallel Connected Dual Converter System without Interphase Reactors", Proceedings of ICEE'98, Vol. 1, pp. 75-79, 1998.

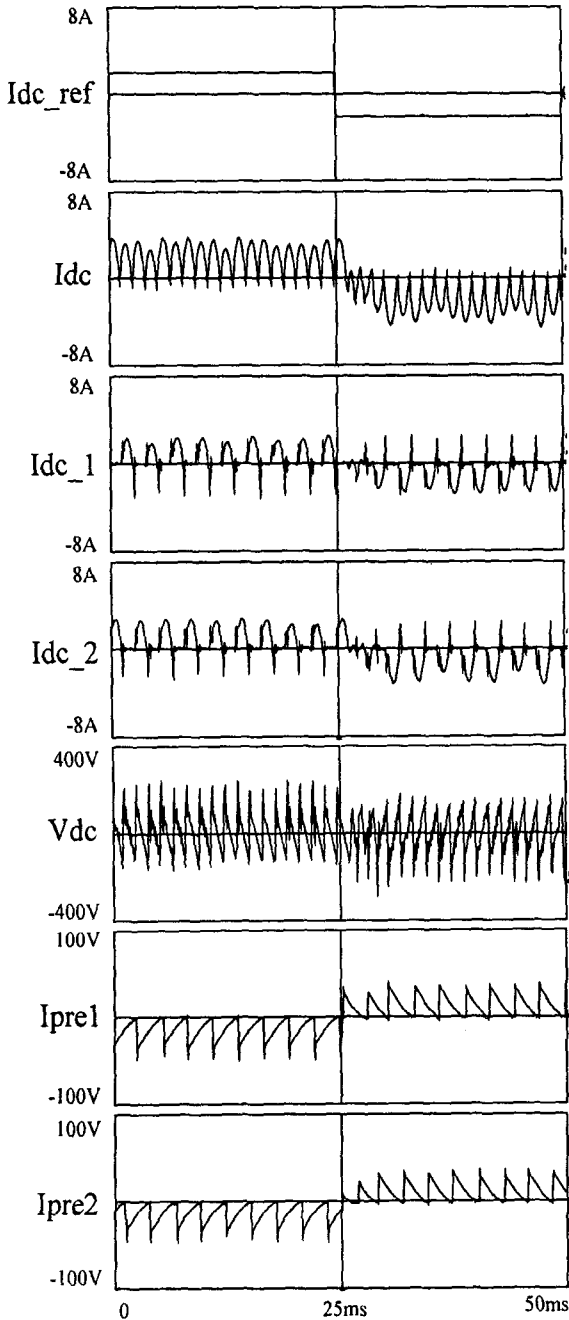


Fig. 6 Predictive current control response in discontinuous current mode(2A and -2A).

the presented system and the excellence of the predictive current control response is proved through the simulation results and experimental results. We are going to apply this system using predictive current control to real large capacity rolling mill DC drive system.

감사의 글

본 논문은 순천향대학교 대학자재연구비 지원에 의하여 수행된 것입니다.

저 자 소 개



지준근 (池俊根)

1964년 2월 10일생. 1986년 2월 서울대 공대 전기공학과 졸업(학사). 1988년 2월 동대학원 전기공학과 졸업(석사). 1994년 2월 동 대학원 전기공학과 졸업(공학).

1991년 3월 - 1994년 8월 기초전력공학공 동연구소 위촉연구원. 1994년 9월 ~ 현재 순천향대 정보기술공학부 조교수

Tel : 041-530-1371, Fax : 041-530-1373

E-mail : jkji@sch.ac.kr